Table 2 Deflection bounds on modes 1 and 2

Station X/R	I Mode, 600 segments, 2 iterations UB	Runge-Kutta method	LB	II Mode, 600 segments, 2 iterations UB	Runge-Kutta method	LB
0.0	0.0000	0.0000	0.0000	0.0000	0.0000	0.0000
0.2	0.0871	0.0871	0.0871	−0.2878	−0.2888	−0.2898
0.4	0.2738	0.2738	0.2738	−0.6273	−0.6336	−0.6400
0.6	0.5023	0.5023	0.5023	−0.5144	−0.5393	−0.5641
0.8	0.7485	0.7485	0.7485	0.1759	0.0916	0.0072
1.0	1.000018	1.0000	0.999982	1.2648	1.0000	0.7352

some point on the structure. In the present case a unit tip amplitude of the rotor is specified. In terms of bounds on the transfer matrix elements, bounds on the deflection mode shape $W(x)$ are given by

$$\hat{W}(x) = \hat{t}_{13}\hat{t}_{34}/\hat{D} - \tilde{t}_{14}\tilde{t}_{33}/\hat{D} \text{ where } \hat{D} = \hat{t}_{13}\hat{t}_{34} - \tilde{t}_{14}\tilde{t}_{33}$$

$$\tilde{W}(x) = \tilde{t}_{13}\tilde{t}_{34}/\tilde{D} - \hat{t}_{14}\hat{t}_{33}/\tilde{D} \qquad \tilde{D} = \tilde{t}_{13}\tilde{t}_{34} - \hat{t}_{14}\hat{t}_{33}$$

and

$$\tilde{D} > 0 \tag{13}$$

Note that all upper bounds transfer matrices are evaluated at the upper bound frequency for that mode. Slightly different expressions obtained by using rules given in Ref. 12 are used for the mode shape if $\tilde{D}$ is negative. Bounds for modes 1 and 2 are compared with a Runge-Kutta solution in Table 2. Bounds on the preceding frequencies can also be obtained by a procedure given in Ref. 15, but the method does not provide bounds on the corresponding mode shape which one can obtain by the present approach.

Acknowledgment

This research was sponsored by the National Science Foundation under Grant GK-40589 and by the Iowa State University Engineering Research Institute.

References

[1]Pestel, E. C. and Leckie, F. A., *Matrix Methods in Elastomechanics*, McGraw-Hill, New York, 1963.

[2]Lin, Y. K., *Probablistic Theory of Structural Dynamics*, McGraw-Hill, New York, 1963.

[3]McDaniel, T. J. and Henderson, J. P., "Review of Transfer Matrix Vibration Analysis of Skin Stringer Structure," *The Shock and Vibration Digest*, Vol. 6, No. 1 (Part I), Vol. 6, No. 2 (Part II), 1974.

[4]Lin, Y. K. and McDaniel, T. J., "Dynamics of Beam-Type Periodic Structures," *Journal of Engineering for Industry*, Vol. 91, 1969, pp. 1133–1141.

[5]Murthy, V. R. and Pierce, G. A., "Effect of Phase Angle on Multibladed Rotor Flutter," to be published in *Journal of Sound and Vibration*.

[6]Murthy, V. R., "Dynamic Characteristics of Rotor Blades," to be published in *Journal of Sound and Vibration*.

[7]Murthy, V. R. and Nigam, N. C., "Dynamic Characteristics of Stiffened Rings by Transfers Matrix Approach," *Journal of Sound and Vibration*, Vol. 39, No. 2, March 1975, pp. 237–245.

[8]Walter, W., *Differential and Integral Inequalities*, Springer-Verlag, New York, 1970.

[9]Protter, M. H. and Weinberger, H. S., *Maximum Principles in Differential Equations*, Prentice-Hall, Englewood Cliffs, New Jersey, 1967.

[10]Lakshmikantham, V., and Leela, S., *Differential and Integral Inequalities*, Vol. 1, *Ordinary Differential Equations*, Academic Press, New York and London, 1969.

[11]McDaniel, T. J. and Murthy, V. R., "Solution Bounds for Varying Geometry Beams," to appear in the *Journal of Sound and Vibration*.

[12]Murthy, V. R. and McDaniel, T. J., "Solution Rounds to Structural Systems," *AIAA Journal*, Vol. 14, Jan. 1976, pp. 111–113.

[13]Hubolt, J. C. and Brooks, G. W., "Differential Equations of Motion for Combined Flapwise Bending, Chordwise Bending, and Torsion of Twisted, Non-Uniform Rotor Blades," NASA Rep. 1346, 1958.

[14]Murthy, V.R., "Determination of Structural Dynamic Characteristics of Rotor Blades and the Effect of Phase Angle on Multi-bladed Rotor Flutter," Ph.D. dissertation, Georgia Institute of Technology, 1974.

[15]Bazley, N. W. and Fox, D. W., "Lower Bounds to Eigenvalues Using Operated Decompositions of the Form B*B," *Archive for Rational Mechanics and Analysis*, Vol. 10, 1962, pp. 352–360.

Rocket Nozzle Damping Characteristics Measured Using Different Experimental Techniques

B. A. Janardan* and B. T. Zinn†
Georgia Institute of Technology, Atlanta, Ga.

Introduction

In linear stability considerations of rocket motors, it is customary to evaluate the effect of the nozzle on the growth or decay rate of a small-amplitude oscillation inside the combustor by determining the nozzle decay coefficient. When the nozzle is the only factor that affects the combustor oscillation, the temporal behavior of the oscillation in terms of the nozzle decay coefficient α_N can be expressed in the following form:

$$P_1(z,t) = P(z)e^{(\alpha_N t)}e^{(i\omega t)}$$

To date, several experimental techniques have been developed for the determination of the values of α_N of rocket nozzles. It is the objective of this investigation to determine the decay coefficient α_N of a small-scale solid rocket exhaust nozzle by all of the available experimental methods and to compare the data so obtained with one another and with available empirical and theoretical nozzle damping data. The measured data are presented in this note, together with a brief review of the techniques used to measure α_N.

Experimental Techniques

An apparatus commonly employed to measure the rocket nozzle damping data is illustrated in Fig. 1. It consists of a simulated cold flow chamber with the test nozzle at one end and an injector plate at the other end. Using this apparatus, the nozzle damping characteristics have been measured employing several techniques.[1-4] These are referred to as the wave-attenuation, frequency-response, and standing-wave methods. These methods are reviewed briefly below, together with a discussion on their applicability for the determination of α_N.

Received Nov. 16, 1976.

Index categories: Combustion Stability, Ignition, and Detonation; Solid and Hybrid Rocket Engines.

*Research Engineer, School of Aerospace Engineering.

†Regents' Professor of Aerospace Engineering. Associate Fellow AIAA.

Wave-Attenuation Method

In the wave-attenuation or decay technique,[1] a standing-wave pattern at the frequency of one of the natural modes of the simulated combustor is excited in the simulated combustor containing a one-dimensional mean flow. During a test, the time history of the pressure amplitude at a given location is measured continuously after switching off the acoustic driver, and from these data the nozzle decay coefficient is determined. Implied in this measurement technique[4] is the assumption that the mode shapes of the simulated chamber are not very much different from the closed-chamber mode shapes. This is true only for small values of mean flow Mach number and chamber end admittances. In addition, it is assumed that the acoustic attenuation associated with the injector end of the chamber is negligible and that the observed decay is due solely to the nozzle.

Frequency-Response Method

In the frequency-response or steady-state resonance technique,[1] an acoustic wave of a known frequency is excited in the simulated cold-flow combustor. The frequency of the oscillations is varied slowly over a range of frequencies, starting with a frequency below one of the resonant frequencies of the chamber and ending at a frequency above the chosen resonant frequency. The amplitudes of the resulting pressure oscillations at a given location are measured and plotted as a function of the frequency. From the shape of the resulting acoustic response curve, the nozzle decay coefficient at the chosen resonant frequency is deterimined by a procedure described in Ref. 4. This method assumes that the acoustic output of the driver is independent of the frequency, a situation rather difficult to achieve in practice. In addition, the application of this method is limited to nozzle configurations whose admittances vary slowly with frequency.

Standing-Wave Method

In the standing-wave or modified impedance-tube method[2,3] a standing wave of the desired frequency is superimposed on the mean flow present in the simulated rocket combustor. The nozzle admittance is determined by measuring the axial distribution of the amplitudes and/or phases of the resulting steady-state standing wave. The nozzle decay coefficient then is determined by substituting the measured admittance into the expressions derived by Cantrell and Hart.[5] The standing-wave method, unlike the other two methods just mentioned, is not restricted to the determination of nozzle damping data at the resonant frequencies of the simulated chamber only. In addition, this method has none of the limitations of the frequency-response and wave-attenuation techniques.

Results

During this investigation, the frequency dependence of the decay coefficients of a geometrically similar small-scale solid rocket nozzle has been measured independently employing the three earlier mentioned techniques. The test configuration, shown in Fig. 1, has a nozzle area ratio J (defined as the ratio of the nozzle throat area to the chamber cross-sectional area) equal to 0.138. The measured data have been obtained under cold flow conditions and over a frequency range of 50 to 400 Hz. The details of the experimental facility are given in Refs. 2 and 3.

The measured frequency dependence of the nondimensional decay coefficient Λ_N of the small-scale nozzle is presented in Fig. 2 as a function of the nondimensional frequency F. The quantities Λ_N and F are defined as $\Lambda_N = \alpha_N L_C/\bar{c}$ and $F = 2\pi f L_N/\bar{c}$, where f is the test frequency in Hertz, L_C and L_N are, respectively, the lengths of the combustor and the convergent section of the nozzle, and $\bar{c}$ is the steady-state velocity of sound. An examination of Fig. 2

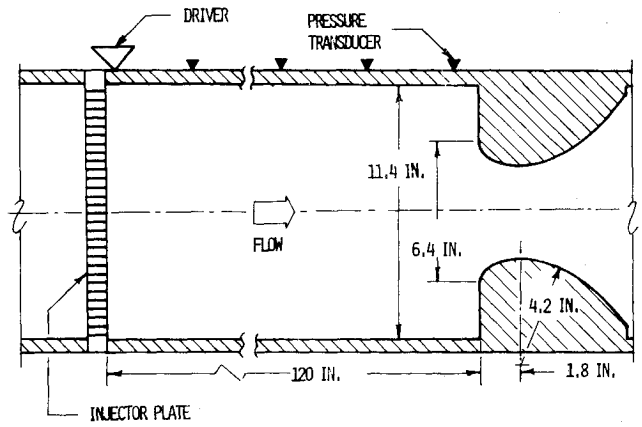

Fig. 1 Simulated cold-flow rocket combustor with the test nozzle.

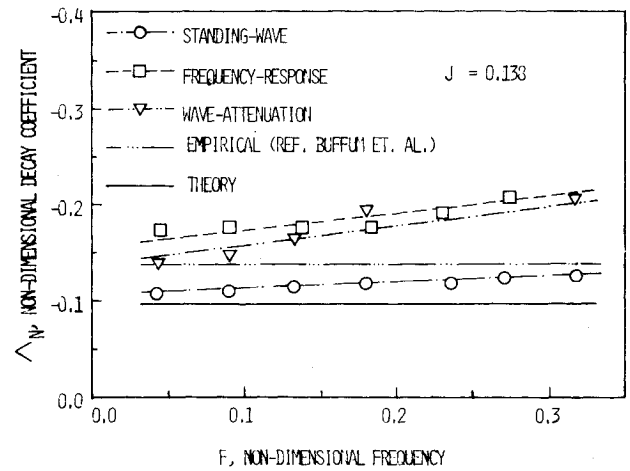

Fig. 2 Nondimensional decay coefficients of the test nozzle.

indicates that, although all of the measurement techniques yield values of Λ_N of comparable magnitudes, the nozzle decay data obtained using the standing-wave technique are lower than those measured during the frequency-response and wave-attenuation tests. This observed difference in the decay coefficients is not unexpected in view of the limitations and assumptions involved with the use of the frequency-response and wave-attenuation methods. As stated earlier, the frequency-response and wave-attenuation measurement techniques are based upon the assumption that the observed decay is due solely to nozzle damping and that the acoustic attenuation associated with the injector end of the chamber is negligible. This is rather a questionable assumption, particularly when the measured decay data are small in magnitude, as is the case in the present investigation.

For comparison, the nozzle decay coefficient calculated by using the empirical relation $\Lambda_N = -J$, obtained by Buffum et al.,[1] also is shown in Fig. 2. It needs, however, to be pointed out that this empirical relation was arrived at from damping data of short nozzles measured by the use of the frequency-response and wave-attenuation methods. Furthermore, the damping data of Ref. 1 were measured only at the first longitudinal resonant frequency of the simulated motor chamber. Indeed, an examination of Fig. 2 indicates that, at the fundamental (i.e., $1L$), resonant frequency of the simulated combustor, the decay data measured during the present investigation by the use of frequency-response and wave-attenuation methods agree with Buffum's data.[1]

Figure 2 also contains a comparison of the measured data with the theoretical predictions of Ref. 6. Assuming that the convergent section of the nozzle is short relative to the wavelength and that the nozzle flow in it is both isoenergetic and isentropic, Ref. 6 uses a quasisteady theory to derive an

expression for the short nozzle admittance that is frequency independent. Substituting this expression for the nozzle admittance into the relationship derived by Cantrell and Hart,[5] the theoretical formula $\Lambda_N = -\bar{M}\ (\gamma+1)/2$ is obtained, where γ is the specific heat ratio and $\bar{M}$ is the mean flow Mach number in the chamber. Letting $\gamma = 1.4$, the theoretically predicted value of Λ_N for the test nozzle has been calculated, and it also is presented in Fig. 2. A comparison of the predicted and measured values of Λ_N shows that the predicted data are lower than the corresponding measured values and that the data obtained from the standing-wave method are in best agreement with the theoretical predictions.

It is believed that the main reason for the observed discrepancy between the theoretical and experimental results is that the cross-sectional areas of the combustor and the test nozzle are not equal in the experimental setup (see Fig. 1 for details). Consequently, the flow stream separates from the simulated chamber walls at some location upstream of the nozzle entrance plane which results in a nonuniform steady flow region just upstream of the nozzle entrance plane. This region may result in additional attenuation that is reflected in the measured values of Λ_N. The losses associated with the nonuniform flow region are not accounted for in the theoretical analysis of Ref. 6, and hence the predicted value of Λ_N accounts for damping provided by the nozzle only.

It obviously is desirable to have the capability for separating the acoustic losses associated with the nozzle and the region of nonuniform flow just upstream of the nozzle entrance. One way to obtain such data is to compare the data reported in this note with decay data obtained when the tested nozzle smoothly connects into the simulated combustor. As no such tests were conducted during this investigation, the aforementioned comparison cannot be carried out. However, useful observations can be made by considering the data reported in Ref. 2. In this study, the admittances of a family of liquid rocket nozzles whose entrance areas equaled the cross-sectional area of the simulated combustor have been measured and compared with the theoretical predictions of the Crocco's nozzle admittance theory.[7] An examination of the data presented in Ref. 2 (i.e., see Figs. 4-6 of Ref. 2) indicates a good agreement between the theoretically predicted and experimentally measured data.

The predictions of Crocco's nozzle admittance theory asymptotically approach those of the quasisteady short nozzle theory in the limit when the length of the convergent section of the nozzle is much smaller than the wavelength of the oscillation. Hence, the observed agreement[2] between the measured and predicted nozzle admittance data throughout the frequency range strongly suggests that the short nozzle theory also can be expected to predict the acoustic characteristics of short nozzles that smoothly connect with the combustor. This discussion also suggests that the observed discrepancy between the measured and predicted data can be due to the manner in which the nozzle is attached to the combustor. This further indicates that caution must be exercised whenever available theories are used to predict the admittances and decay data of nozzles having complex geometries in the vicinity of the nozzle entrance plane.

Acknowledgment

The authors acknowledge the assistance provided by B. R. Daniel while conducting the experiments.

References

[1] Buffum, F. G., Dehority, G. L., Slates, R. O., and Price, E. W., "Acoustic Attenuation Experiments on Subscale Cold-Flow Rocket Motors," *AIAA Journal*, Vol. 5, Feb. 1967, pp. 272-280; also "Aconstic Ahenuation in Resonant Model-Rocket Motors," ICRPG/AIAA 2nd Propulsion Conference, AIAA, New York, 1967, pp. 173-180.

[2] Bell, W. A., Daniel, B. R., and Zinn, B. T., "Experimental and Theoretical Determination of the Admittances of a Family of Nozzles Subjected to Axial Instabilities," *Journal of Sound and Vibration*, Vol. 30, Sept. 1973, pp. 179-190.

[3] Janardan, B. A., Daniel, B. R., and Zinn, B. T., "Scaling of Rocket Nozzle Admittances," *AIAA Journal*, Vol. 13, July 1975, pp. 918-923.

[4] Culick, F. E. C. and Dehority, G. L., "Analysis of Axial Acoustic Waves in a Cold-Flow Rocket," *Journal of Spacecraft and Rockets*, Vol. 6, May 1969, pp. 591-595.

[5] Cantrell, R. H. and Hart, R. W., "Interaction Between Sound and Flow in Acoustic Cavities; Mass, Momentum and Energy Considerations," *Journal of the Acoustic Society of America*, Vol. 36, April 1964, pp. 697-706.

[6] Crocco, L. and Sirignano, W. A., "Effect of Transverse Velocity Components on the Non-linear Behavior of Short Nozzles," *AIAA Journal*, Vol. 4, Aug. 1966, pp. 1428-1430.

[7] Crocco, L. and Sirignano, W. A., "Behavior of Supercritical Nozzles Under Three Dimensional Oscillatory Conditions," AGARDograph 117, Princeton Univ., Princeton N. J., 1967.

Numerical Solution for Subcritical Flows by a Transonic Integral Equation Method

Wandera Ogana*
NASA Ames Research Center, Moffett Field, Calif.

Introduction

THE integral equation for two-dimensional transonic flows[1-3] involves a singular kernel. Numerical solution of the equation has been attempted by various methods.[2-7] A major computational challenge concerns the proper treatment of the singular kernel so as to represent accurately the contribution from the double integral. In some schemes,[2,3,5] the double integral is reduced to a line integral over the airfoil by representing the transverse variation of the velocity in terms of the velocity on the airfoil surface, using an arbitrary approximation function that attenuates away from the airfoil. Solutions are obtained only on the airfoil. Radbill[4] and Nixon[6,7] extend the idea of approximation functions to enable computation of flow field values.

For the method presented in this article, the region of integration is divided into closed rectangular elements, and the velocity is taken to be constant in each element. The integral equation is then reduced to a matrix equation solvable by some suitable iteration scheme.

Derivation and Solution of the Matrix Equation

Let $\bar{\delta}$ be the thickness ratio of a thin airfoil, in the physical rectangular coordinates $(\bar{x},\bar{y})$, whose upper profile is described by $\bar{y}=\bar{Y}_+(\bar{x})$ and lower profile by $\bar{y}=\bar{Y}_-(\bar{x})$. For a freestream Mach number, $M_\infty < 1$, and a transonic similarity parameter, $\underline{K}=(1-M_\infty^2)/M_\infty^{4/3}\bar{\delta}^{2/3}$, the coordinate transformations, $x=\bar{x}$ and $y=(1-M_\infty^2)^{1/2}\bar{y}$, enable the integral equation to be written in the form[1]

$$u(x,y) = u_B(x,y) + \nu u^2(x,y) + \int_S\int \kappa(\xi-x,\zeta-y)\,u^2(\xi,\zeta)\,dS \tag{1}$$

where

$$\kappa(\xi-x,\zeta-y) = -\frac{(\xi-x)^2-(\zeta-y)^2}{4\pi[(\xi-x)^2+(\zeta-y)^2]^2} \tag{2a}$$

$$\nu = (1/\pi)\arctan(\lambda) \tag{2b}$$

Received Oct. 21, 1976.
Index category: Subsonic and Transonic Flow.
*NRC Research Associate.